

## $\tau$ Binds and Organizes *Escherichia coli* Replication Proteins through Distinct Domains

DOMAIN IV, LOCATED WITHIN THE UNIQUE C TERMINUS OF  $\tau$ , BINDS THE REPLICATION FORK HELICASE, DnaB\*

Received for publication, October 27, 2000

Published, JBC Papers in Press, November 14, 2000, DOI 10.1074/jbc.M009830200

Dexiang Gao and Charles S. McHenry

From the Department of Biochemistry and Molecular Genetics and Program in Molecular Biology, University of Colorado Health Sciences Center, Denver, Colorado 80262

**Interaction between the  $\tau$  subunit of the DNA polymerase III holoenzyme and the DnaB helicase is critical for coupling the replicase and the primosomal apparatus at the replication fork (Kim, S., Dallmann, H. G., McHenry, C. S., and Marians, K. J. (1996) *Cell* 84, 643–650). In the preceding manuscript, we reported the identification of five putative structural domains within the  $\tau$  subunit (Gao, D., and McHenry, C. (2000) *J. Biol. Chem.* 275, 4433–4440). As part of our systematic effort to assign functions to each of these domains, we expressed a series of truncated, biotin-tagged  $\tau$  fusion proteins and determined their ability to bind DnaB by surface plasmon resonance on streptavidin-coated surfaces. Only  $\tau$  fusion proteins containing domain IV bound DnaB. The DnaB-binding region was further limited to a highly basic 66-amino acid residue stretch within domain IV. Unlike the binding of immobilized  $\tau_4$  to the DnaB hexamer, the binding of monomeric domain IV to DnaB<sub>6</sub> was dependent upon the density of immobilized domain IV, indicating that DnaB<sub>6</sub> is bound by more than one  $\tau$  protomer. This observation implies that both the leading and lagging strand polymerases are tethered to the DnaB helicase via dimeric  $\tau$ . These double tethers of the leading and lagging strand polymerases proceeding through the  $\tau$ - $\tau$  link and an additional  $\tau$ -DnaB link are likely important for the dynamic activities of the replication fork.**

replicase with the primosome and mediate rapid replication fork movement (10, 11). These two important functions of  $\tau$  reside in C- $\tau$ , a proteolytic fragment consisting of its unique C-terminal 213 amino acid residues.  $\tau$  binds tightly to the  $\alpha$  subunit; the shorter translation product  $\gamma$  does not. C- $\tau$  is a monomer and binds  $\alpha$  with a 1:1 stoichiometry as determined by sedimentation equilibrium analyses (12). Results from a recent study indicated that C- $\tau$  binds DnaB, can partially replace full-length  $\tau$  in reconstituted rolling circle replication reactions, and effectively couples the leading strand polymerase with DnaB helicase at the replication fork (12). DnaB helicase is composed of six identical subunits and is a stable hexamer over a wide range of concentration in the presence of magnesium ions (13, 14).

In the preceding manuscript, we reported that  $\tau$  comprises five potential structural domains (15). Domains I, II, and III are common to both  $\gamma$  and  $\tau$ . Domain IV includes 66 amino acid residues of the C- $\tau$  sequence and the C-terminal 17 residues of  $\gamma$ . Domain V corresponds to the 147 C-terminal residues of the  $\tau$  subunit. Based on these assignments, biotin-hexahistidine-tagged  $\tau$  proteins lacking specific domains were produced. Results from binding studies employing these truncated fusion proteins indicated that the binding site of  $\tau$  for  $\alpha$  subunit lies within its C-terminal 147 amino acid residues (domain V).

The objective of this study was to determine the domain(s) of the  $\tau$  subunit involved in binding DnaB. Biotin-hexahistidine-tagged  $\tau$  proteins lacking specific domains were expressed and purified. Analysis of DnaB binding to these truncated  $\tau$  proteins by surface plasmon resonance permitted the assignment of the DnaB-binding domain of  $\tau$ .

### EXPERIMENTAL PROCEDURES

**Strains**—*E. coli* DH5 $\alpha$  and HB101 were used for initial molecular cloning procedures and plasmid propagation. *E. coli* BL21( $\lambda$  DE3) was used for protein expression.

**Buffers**—Buffer L, Buffer W and HKGM Buffer were prepared as previously described (15).

**Chemicals and Reagents**—SDS-polyacrylamide gel electrophoresis protein standards were obtained from Amersham Pharmacia Biotech, and prestained molecular mass markers were from Bio-Rad or Life Technologies, Inc. Ni<sup>2+</sup>-NTA<sup>1</sup> resin, QIAquick Gel extraction kits, QIAquick PCR purification kits, and plasmid preparation kits were purchased from Qiagen. The Coomassie Plus protein assay reagent and ImmunoPure Streptavidin were from Pierce. CM5 sensor chips (research grade), P-20 surfactant, N-hydroxysuccinimide, 1-ethyl-3-[(3-dimethylamino)propyl] carbodiimide, and ethanolamine hydrochloride were obtained from BIAcore Inc.

**Proteins**—Three biotin-tagged  $\tau$  proteins C(0) $\tau$ , C- $\Delta$ 147 $\tau$ , and

The DNA polymerase III holoenzyme is responsible for the replication of the *Escherichia coli* chromosome. Like other replicases from eukaryotes and prokaryotes, the holoenzyme contains three functional subassemblies (for reviews see Refs. 1–3): the DNA polymerase III ( $\alpha\epsilon\theta$ ) core, the  $\beta$  sliding clamp processivity factor, and the DnaX complex, a clamp assembly apparatus. The DNA polymerase III core contains the  $\alpha$ ,  $\epsilon$ , and  $\theta$  subunits and provides the polymerase function. The DnaX complex ( $\tau_2\gamma\delta\delta'\chi\psi$ ) is a multiprotein ATPase that recognizes the primer terminus and loads the  $\beta$  processivity factor onto DNA.

The  $\tau$  and  $\gamma$  subunits are different translation products of the *dnaX* gene (4–7). The  $\tau$  subunit plays central roles in the structure and function of the holoenzyme. It interacts with the core polymerase to coordinate leading and lagging strand synthesis (8, 9).  $\tau$  also interacts with DnaB helicase to couple the

\* This work was supported by Grant GM36255 from the National Institutes of Health. The costs of publication of this article were defrayed in part by the payment of page charges. This article must therefore be hereby marked "advertisement" in accordance with 18 U.S.C. Section 1734 solely to indicate this fact.

<sup>1</sup> The abbreviations used are: NTA, nitrilotriacetic acid; PCR, polymerase chain reaction; RU, resonance unit.

TABLE I  
Oligonucleotides used for construction of truncated  $\tau$  fusion proteins

Oligonucleotide number	Use	Sequence <sup>a</sup>
C-213p1	C- $\Delta$ 213 $\tau$	<u>TACAAC</u> TTTCGCCTGCTGC <u>ACTTG</u>
C-213p2	C- $\Delta$ 213 $\tau$	GGACTAGTACTCTTTTTTTGGCTTTGGTTGCTCCC
N-430p1	N- $\Delta$ 430 $\tau$	AACTGCAGAAAGAGTGAACCGGCAGCC
N-430p2	N- $\Delta$ 430 $\tau$	CTCGCATGGGGAGACCCACAC

<sup>a</sup> The underlined regions are complementary to the DnaX gene sequence on the template.

N- $\Delta$ 413 $\tau$  as well as holoenzyme subunits were prepared as previously described (15).

**Construction of the Fusion Plasmids**—Plasmids P<sub>A1</sub>-C- $\Delta$ 213 $\tau$  and pET11-N- $\Delta$ 430 $\tau$  were constructed to express the fusion proteins C- $\Delta$ 213 $\tau$  and N- $\Delta$ 430 $\tau$ , respectively. Fusion protein C- $\Delta$ 213 $\tau$  corresponds to  $\gamma$ , the shorter of the two potential *dnaX* products. In this construct, the 213 C-terminal residues found exclusively in the  $\tau$  subunit are replaced by a peptide tag, which includes hexahistidine and a 13-amino acid residue biotinylation sequence. N- $\Delta$ 430 $\tau$  corresponds to C- $\tau$ ; the N-terminal 430 amino acids found in both  $\tau$  and  $\gamma$  are replaced by the hexahistidine/biotinylation tag. P<sub>A1</sub> is a semi-synthetic *E. coli* RNA polymerase-dependent promoter containing two *lac* operators (16). The pET11 vector is under the control of the T7 promoter.

The starting material for construction of plasmid P<sub>A1</sub>-C- $\Delta$ 213 $\tau$  was P<sub>A1</sub>-C(0) $\tau$ , which encodes the C-terminal tagged full-length  $\tau$  protein (15). PCR primer C-213P1 (Table I) is complementary to a 110-nucleotide stretch upstream of the *RsrII* site within *dnaX*. Primer C-213P2 (Table I) corresponded to *dnaX* codons 423–430 preceded by a non-complementary *SpeI* restriction site. P<sub>A1</sub>-C(0) $\tau$  was digested with *RsrII* and *SpeI*. The PCR product generated by use of primers C-213P1/C-213P2 was cleaved with *RsrII* and *SpeI* and then ligated into the linearized vector to generate plasmid P<sub>A1</sub>-C- $\Delta$ 213 $\tau$ .

Primers N-430p1 and N-430p2 (Table I) and plasmid P<sub>A1</sub>-N- $\Delta$ 1 $\tau$ , which encodes an N-terminal tagged  $\tau$  protein (15), were used to generate a PCR product for the construction of pET11-N- $\Delta$ 430 $\tau$ . The resultant PCR product consisted of a *PstI* restriction site within the non-complementary 5' region followed by *dnaX* codons 431–436 and a *KpnI* site near the 3' end. The *KpnI* site located downstream of the natural *dnaX* stop codon. After digestion with *PstI* and *KpnI*, the resultant 929-base pair fragment was used to replace the *dnaE* gene of vector pET11-N0 (16) to produce plasmid pET11-N- $\Delta$ 430 $\tau$ .

**Growth and Induction of Expressing *E. coli* Strains**—*E. coli* strain BL21 ( $\lambda$  DE3) containing the expression plasmids pET11-N- $\Delta$ 430 $\tau$  or P<sub>A1</sub>-C- $\Delta$ 213 $\tau$  was grown at 37 °C in 2 and 6 liters, respectively, of F medium (17) containing 100  $\mu$ g/ml ampicillin. Cells were induced with isopropyl- $\beta$ -D-thio-galactoside, biotin-treated, and harvested as described (15).

**Protein Purification**—The procedures for purification of C- $\Delta$ 213 $\tau$  and N- $\Delta$ 430 $\tau$  were similar to those described for other truncated  $\tau$  fusion proteins (15). Briefly, induced cells (14 g for C- $\Delta$ 213 $\tau$  or 22 g for N- $\Delta$ 430 $\tau$ ) were lysed in the presence of lysozyme (2.5 mg/ml), EDTA (5 mM), benzamidine (5 mM), and phenylmethylsulfonyl fluoride (1 mM) for 2 h at 4 °C and 6 min at 37 °C. For purification of C- $\Delta$ 213 $\tau$ , 0.226 g of ammonium sulfate was added to each milliliter of the resulting supernatant, and the precipitate was collected by centrifugation at 23,300  $\times$  g at 4 °C for 1 h. The pellets were then resuspended in Buffer L. Each suspension was mixed with 1 ml of Ni<sup>2+</sup>-NTA resin and pre-equilibrated with Buffer L, and the slurries were then packed into 1-ml columns. Columns were washed with ~30 column volumes of buffer W containing 23 mM imidazole. Bound proteins were then eluted with buffer W containing 150 mM imidazole in a single step. 13 mg of C- $\Delta$ 213 $\tau$  were obtained in the preparation used for these studies. The purification of N- $\Delta$ 430 $\tau$  was as that for C- $\Delta$ 213 $\tau$  except that: 1) the supernatant proteins were precipitated with 65% ammonium sulfate, 2) 3 ml of pre-equilibrated Ni<sup>2+</sup>-NTA resin were used, 3) the columns were washed with buffer W containing 10 mM imidazole, and 4) elutions were effected by a 10–100 mM imidazole gradient in buffer W. 61 mg of purified N- $\Delta$ 430 $\tau$  were obtained in the preparation used for these studies.

**Surface Plasmon Resonance**—A BIAcore™ instrument was used for protein-protein binding studies. Research grade CM5 sensor chips were used in all experiments. Streptavidin was captured onto sensor chips by *N*-hydroxysuccinimide/1-ethyl-3-[(3-dimethylamino)propyl] carbodiimide coupling as previously described (15). The biotinylated  $\tau$  proteins were then injected over the immobilized streptavidin sensor chip. Binding analyses of  $\tau$  to DnaB (0.025–1  $\mu$ M) were performed in HXGM buffer at 20 °C. Kinetic parameters were determined using the BIAevaluation™ 2.1 software.

**Other Procedures**—DNA polymerization assays, protein determinations, and SDS-polyacrylamide gel electrophoresis were performed as described in the preceding paper (15).

## RESULTS

**Expression and Purification of the Truncated  $\tau$  Fusion Proteins**—The  $\tau$  subunit binds to DnaB helicase and is the only subunit within the holoenzyme shown to interact with DnaB (10). The unique C terminus of  $\tau$  (C- $\tau$ ) bound DnaB in a coupled immunoblotting method (12). To confirm this observation and more precisely map the DnaB binding region of  $\tau$ , a series of truncated  $\tau$  proteins lacking specific domains were produced, and their interactions with DnaB helicase were quantified using BIAcore methodology. The  $\tau$  fusion proteins employed in this study included C(0) $\tau$  (domains I-V), C- $\Delta$ 147 $\tau$  (domains I-IV), C- $\Delta$ 213 $\tau$ , which was equivalent to  $\gamma$  (domains I-III plus 17 amino acids of domain IV), N- $\Delta$ 413 $\tau$  (domains IV and V), and N- $\Delta$ 430 $\tau$ , which was equivalent to C- $\tau$  (the C-terminal 66 residues of domain IV plus domain V in its entirety). The truncated terminus of each fusion protein was tagged with a peptide containing both a hexahistidine sequence to aid in purification as well as a short biotinylation sequence. The biotinylation sequence enabled oriented immobilization of the fusion proteins onto BIAcore sensor chips via biotin-streptavidin binding. C(0) $\tau$ , C- $\Delta$ 147 $\tau$ , and N- $\Delta$ 413 $\tau$  were expressed and purified as previously described (15). C- $\Delta$ 213 $\tau$  and N- $\Delta$ 430 $\tau$  were expressed in the BL21 ( $\lambda$  DE3) strain by induction with isopropyl- $\beta$ -D-thio-galactoside and reached similar expression levels (2–5% of total cell proteins). Both C- $\Delta$ 213 $\tau$  and N- $\Delta$ 430 $\tau$  were purified by Ni<sup>2+</sup>-NTA affinity chromatography. After Ni<sup>2+</sup>-NTA purification, C- $\Delta$ 213 $\tau$  was obtained at 80% purity, and N- $\Delta$ 430 $\tau$  at 90% purity as determined by SDS-polyacrylamide gel electrophoresis analysis (Fig. 1). The activities of the fusion proteins were ascertained by their ability to replace  $\gamma$  or  $\tau$  in DNA polymerase III reconstitution assays (15). The specific activity of C- $\Delta$ 213 $\tau$  was  $5.5 \times 10^6$  units/mg, similar to that of full-length C(0) $\tau$  ( $5.7 \times 10^6$  units/mg). As expected, no holoenzyme reconstitution activity was detected for N- $\Delta$ 430 $\tau$ , which lacks the  $\gamma$  sequence required for assembly of the  $\beta$  processivity factor on DNA.

**DnaB Binding to  $\tau$  Proteins Containing Domain IV**—The interaction between DnaB and C(0) $\tau$  was first characterized via use of BIAcore technology. C(0) $\tau$  (2025 RU) was immobilized onto a streptavidin sensor chip. DnaB solutions of varying concentrations were passed over the immobilized C(0) $\tau$ , and binding activity was monitored (Fig. 2A). Attempts to fit the dissociation phase to a single first-order dissociation equation were unsuccessful, suggesting that a more complex mechanism was operative. To simplify the kinetic analysis, a limited interval (35–125 s following the starting point of dissociation) was analyzed from each binding curve and fit to a model in which two simultaneous independent dissociation processes occur. The two apparent dissociation rate constants  $k_{\text{off major}}$  and  $k_{\text{off minor}}$  (Table II) corresponded to 70–80% and 20–30% of the dissociating species, respectively.  $k_{\text{off major}}$  was used to calculate the apparent association rate ( $k_{\text{on}}$ ). The apparent  $K_d$  was calculated from  $k_{\text{on}}$  and  $k_{\text{off}}$ . The interaction between DnaB and C(0) $\tau$  had an apparent  $K_d$  of 4 nM (Table II). Under the conditions employed in these studies, DnaB is known to exist as a

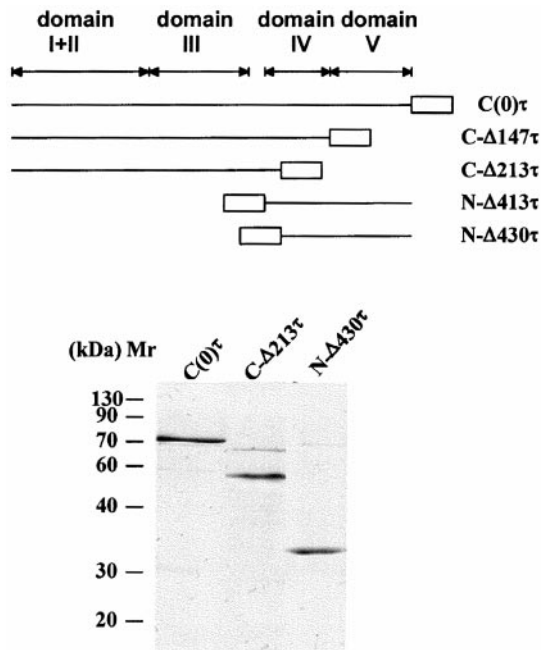


**FIG. 1. Purified truncated  $\tau$  fusion proteins.** The upper panel shows the truncated fusion proteins of  $\tau$  used in this study: C(0) $\tau$  (domain I-V); C- $\Delta$ 147 $\tau$  (domains I-IV); C- $\Delta$ 213 $\tau$  (domains I-III + 17 amino acids of domain IV), which is equivalent to the  $\gamma$  protein plus a C-terminal tag; N- $\Delta$ 413 $\tau$  (domains IV and V); and N- $\Delta$ 430 $\tau$  contains the intact domain V and the majority of domain IV lacking its N-terminal 17-amino acid sequence. The rectangular box represents the fusion peptide. The lower panel is the Coomassie Blue-stained 12% SDS-polyacrylamide gel of 1.5  $\mu$ g of each purified protein after Ni<sup>2+</sup>-NTA chromatography (C- $\Delta$ 147 $\tau$  and N- $\Delta$ 413 $\tau$  were shown in the preceding paper).

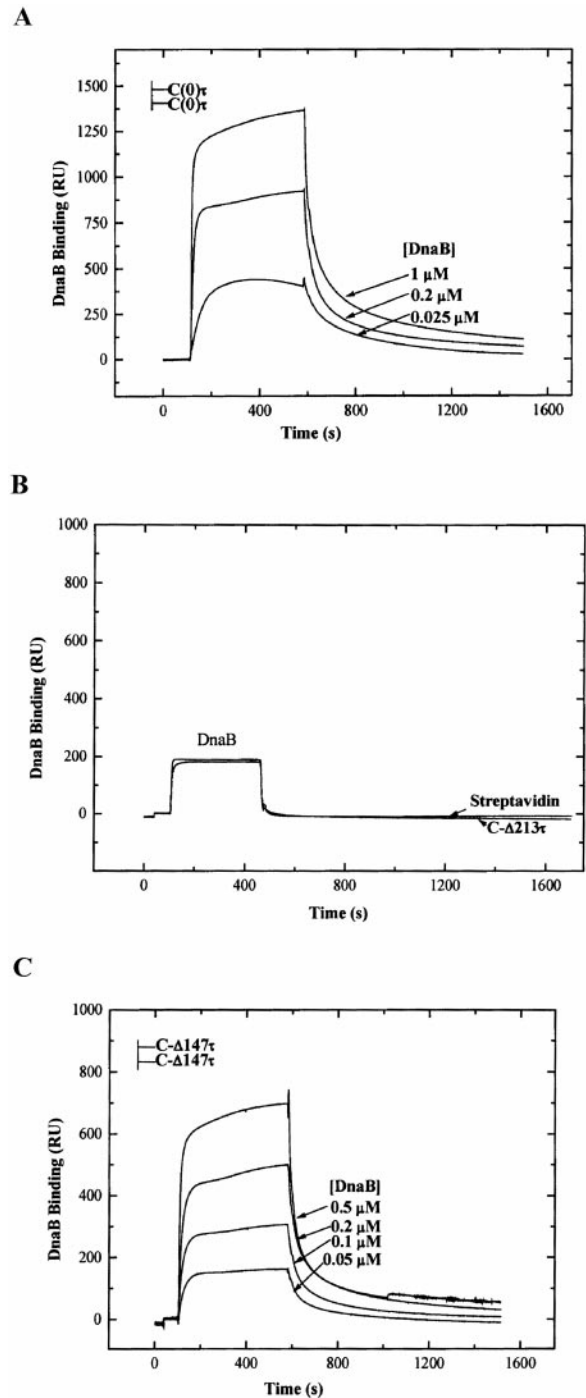
hexamer (14), and C(0) $\tau$  is a tetramer (18). The binding ratio of the DnaB hexamer (DnaB<sub>6</sub>) to the C(0) $\tau$  tetramer [C(0) $\tau$ ]<sub>4</sub> was 0.72, indicating that these multimers likely interact with a 1(DnaB<sub>6</sub>): 1[C(0) $\tau$ ]<sub>4</sub> stoichiometry.

C- $\Delta$ 213 $\tau$ , equivalent to C-terminally tagged  $\gamma$ , was captured onto the streptavidin-derivatized sensor chip (3400 RU), followed by injection of DnaB (1  $\mu$ M). No interaction between C- $\Delta$ 213 $\tau$  and DnaB was detected (Fig. 2B), consistent with the previous finding that  $\gamma$  does not interact with DnaB helicase (10).

Next, DnaB samples (0.05–0.5  $\mu$ M) were injected over immobilized C- $\Delta$ 147 $\tau$  (2860 RU) (Fig. 2C). An apparent  $K_d$  of 5 nM was obtained, which is similar to that of the C(0) $\tau$ -DnaB interaction (Table II). This suggests that C- $\Delta$ 147 $\tau$  contains elements sufficient for binding to DnaB at the same level observed for the intact  $\tau$  subunit. C- $\Delta$ 147 $\tau$  (domains I-IV) bound DnaB, but C- $\Delta$ 213 $\tau$  (domains I-III) did not, localizing the region required for DnaB binding to somewhere within domain IV.

**DnaB Recognizes a 66-Amino Acid Sequence within Domain IV**—To confirm that domain IV was the DnaB-binding domain, N- $\Delta$ 430 $\tau$  (1200 RU) was captured onto a BIAcore sensor chip, and its interaction with DnaB was assessed (Fig. 3A). The dissociation phase did not fit to a single first-order dissociation equation, so the binding data were fit to the model that assumes two parallel dissociation processes. The apparent  $K_d$  was about 8 nM, which was similar to that of the interaction between DnaB and C(0) $\tau$  (Table II). The sum of these results indicates that the DnaB binding site is located within the unique C-terminal 66 residues of the  $\tau$  subunit.

The C-terminal 17 amino acid residues of domain IV are lacking in N- $\Delta$ 430 $\tau$ . To investigate whether these 17 residues provide additional binding energy for the  $\tau$ -DnaB interaction, DnaB binding studies using fusion protein N- $\Delta$ 413 $\tau$  were per-



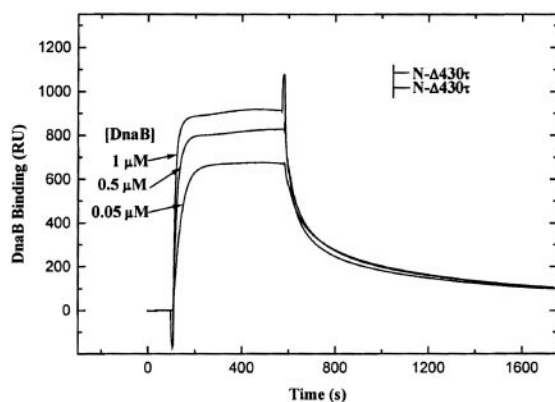
**FIG. 2. DnaB interacts with C(0) $\tau$  and C- $\Delta$ 147 $\tau$  but not C- $\Delta$ 213 $\tau$ .** Streptavidin was chemically immobilized onto sensor chip as described under "Experimental Procedures."  $\tau$  fusion proteins were captured onto the streptavidin sensor chip via biotin-streptavidin interaction. DnaB diluted in H<sub>2</sub>O was injected over immobilized  $\tau$  for 6 min at 5  $\mu$ l/min. Following injection, buffer was passed over the sensor chips for 30 min to permit dissociation of the bound DnaB protein from immobilized  $\tau$  derivatives. A, DnaB interacts with C(0) $\tau$ . 2025 RU of C(0) $\tau$  were captured on the sensor chip, and varying concentrations of DnaB were passed over it. Control injections over a streptavidin sensor chip were performed and subtracted from the data shown. B, DnaB does not interact with C- $\Delta$ 213 $\tau$ . 3390 RU of C- $\Delta$ 213 $\tau$  were captured on the sensor chip, and DnaB at 1  $\mu$ M was injected over the immobilized C- $\Delta$ 213 $\tau$ . The control injection over a streptavidin sensor chip was also shown. C, DnaB interacts with C- $\Delta$ 147 $\tau$ . 2860 RU of C- $\Delta$ 147 $\tau$  were captured onto the streptavidin sensor chip varying concentrations of DnaB were passed over it. Control injections over a streptavidin sensor chip were performed and subtracted from the data shown.

TABLE II  
 Binding of  $\tau$  derivatives to DnaB

$\tau$ derivative	Apparent $k_{on}$	Apparent $k_{off}$		Apparent $K_d^a$	
		Major	Minor		
	$M^{-1} s^{-1}$	$s^{-1}$		$nM$	
C(0) $\tau$	I-V	$7 \times 10^5$	$3 \times 10^{-3}$ (78%)	0.03 (22%)	$4 \pm 0.5$
C- $\Delta$ 147 $\tau$	I-IV	$8 \times 10^5$	$4 \times 10^{-3}$ (72%)	0.04 (28%)	$5 \pm 0.6$
N- $\Delta$ 413 $\tau$	IV, V	$6 \times 10^5$	$3 \times 10^{-3}$ (75%)	0.04 (25%)	$5 \pm 0.4$
N- $\Delta$ 430 $\tau$	IV (80%), V	$6 \times 10^5$	$5 \times 10^{-3}$ (80%)	0.05 (20%)	$8 \pm 0.6$
C- $\Delta$ 213 $\tau$	I-III	No detectable interaction			

<sup>a</sup> Results are the averages of two separate experiments.

A



B

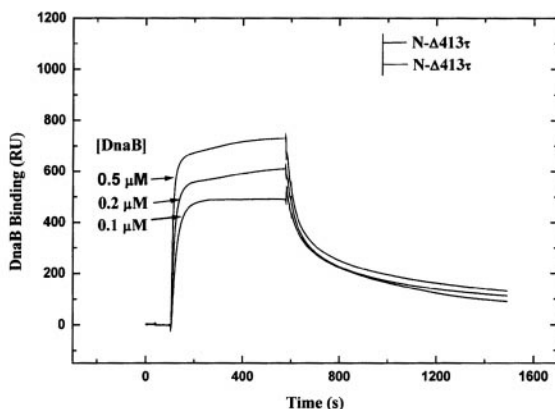


FIG. 3. **N- $\Delta$ 430 $\tau$  and N- $\Delta$ 413 $\tau$  bind DnaB.** Streptavidin was chemically coupled onto the BIAcore sensor chips as described under "Experimental Procedures." 1200 RU of N- $\Delta$ 430 $\tau$  (A) and 1293 RU of N- $\Delta$ 413 $\tau$  (B) were captured onto streptavidin-derivatized sensor chips, and DnaB diluted in HKGM buffer at the indicated concentrations was injected over the chips bearing immobilized N- $\Delta$ 430 $\tau$  and N- $\Delta$ 413 $\tau$ , respectively. Control injections over a streptavidin derivatized sensor chip were performed and subtracted from the data shown.

formed. However, the DnaB/N- $\Delta$ 413 $\tau$  interaction was characterized by an apparent  $K_d$  of 5 nM, which is similar to that observed for the interaction of DnaB with N- $\Delta$ 430 $\tau$  (Fig. 3B and Table II). Thus, it is unlikely that the C-terminal 17 residues of domain IV contribute significantly to DnaB binding interactions.

**More than One  $\tau$  Protomer Binds a DnaB Hexamer**—In the preceding experiment, the binding ratio of DnaB<sub>6</sub> to the monomeric N- $\Delta$ 430 $\tau$  was less than 0.1. This value is significantly different from 0.72, the observed ratio for the interaction between DnaB<sub>6</sub> and C(0) $\tau$ <sub>4</sub>. One potential underlying cause of the low binding ratio for the former interaction is the binding of DnaB<sub>6</sub> to more than one immobilized N- $\Delta$ 430 $\tau$  molecule. To test this hypothesis, we examined the interactions of DnaB (1  $\mu$ M)

TABLE III

Density dependence of N- $\Delta$ 430 $\tau$  binding to DnaB

Immobilized N- $\Delta$ 430 $\tau$		DnaB Bound	Binding ratio (DnaB <sub>6</sub> /(N- $\Delta$ 430 $\tau$ ) <sub>2</sub> ) <sup>b</sup>	
RU	Density <sup>a</sup>	RU		
	$\mu$ M			
146	53	0	0	
368	133	70	0.04	
720	261	315	0.08	
1156	419	937	0.15	
1998	724	2575	0.23	
2700	978	3574	0.24	

Immobilized C(0) $\tau$		DnaB Bound	Binding ratio (DnaB <sub>6</sub> /(C(0) $\tau$ ) <sub>2</sub> ) <sup>b</sup>	
RU	Density	RU		
	$\mu$ M			
2025	270	1437	0.36	
4262	568	5875	0.35	

<sup>a</sup> The concentrations of the immobilized N- $\Delta$ 430 $\tau$  and C(0) $\tau$  were calculated using the following equation (19): concentration (M)  $\equiv$  RU/100  $\times$  molecular weight of the immobilized species ( $M_r$ ).

<sup>b</sup> The binding ratio of the DnaB hexamer to the N- $\Delta$ 430 $\tau$  or C(0) $\tau$  dimer was determined by the following equation: binding ratio = (RU of DnaB bound)/(RU of dimer immobilized)  $\times$  (dimer  $M_r$ )/(DnaB<sub>6</sub> $M_r$ ).

with sensor chips bearing differing amounts of N- $\Delta$ 430 $\tau$  (146 RU-2700 RU). The corresponding densities of the six different levels of N- $\Delta$ 430 $\tau$  tested are shown in Table III. Binding of DnaB to immobilized N- $\Delta$ 430 $\tau$  at 146 RU was not observed. Increased binding ratios of DnaB to N- $\Delta$ 430 $\tau$  were observed for surfaces bearing greater densities of N- $\Delta$ 430 $\tau$  (Fig. 4). If we assume that each DnaB<sub>6</sub> binds two (N- $\Delta$ 430 $\tau$ )<sub>1</sub> molecules, then the binding ratio of DnaB to N- $\Delta$ 430 $\tau$  is increased from 0.04 to 0.24 within the range of the amount of immobilized N- $\Delta$ 430 $\tau$  tested (Table III). The same apparent dissociation and association rate constants for the DnaB and N- $\Delta$ 430 $\tau$  interaction were obtained at different N- $\Delta$ 430 $\tau$  density as reported in Table II. These results are consistent with the multivalent binding of DnaB and N- $\Delta$ 430 $\tau$ . The observed  $K_d$  is the product of the individual  $K_d$  values for single site binding interactions. No binding was observed at low N- $\Delta$ 430 $\tau$  density, suggesting that the monomeric  $\tau$ -DnaB<sub>6</sub> interaction is too weak to be observed with the BIAcore methodology. The apparent  $K_d$  values of the DnaB-N- $\Delta$ 430 $\tau$  interaction and DnaB-C(0) $\tau$  interaction were the same, suggesting that the interaction between DnaB and C(0) $\tau$  is also multivalent; more than one C(0) $\tau$  monomer binds each DnaB<sub>6</sub>. The binding ratio between DnaB and N- $\Delta$ 413 $\tau$  was also N- $\Delta$ 413 $\tau$  density-dependent and increased with increased immobilized N- $\Delta$ 413 $\tau$  density (data not shown).

To ensure that the observed binding ratio of the hexameric DnaB to the tetrameric C(0) $\tau$  was not density-dependent, the binding ratio of DnaB<sub>6</sub> to C(0) $\tau$  was examined at an increased density (4262 RU) of C(0) $\tau$  on a sensor chip. In a previous experiment, 2025 RU of C(0) $\tau$  was used (Fig. 2A), and a binding ratio of 0.72 DnaB<sub>6</sub> to C(0) $\tau$ <sub>4</sub> was observed. The C(0) $\tau$  concentrations in these two different experiments corresponded to 568

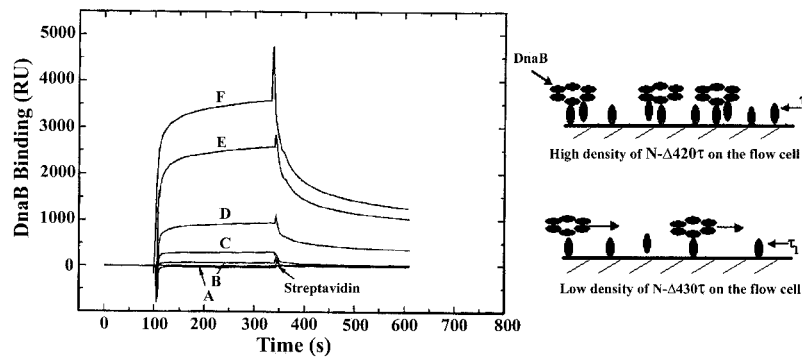


FIG. 4. **N- $\Delta$ 430 $\tau$  density dependence of binding of DnaB.** The left panel shows the interactions of DnaB with six N- $\Delta$ 430 $\tau$  derivatized sensor chips: A, 146 RU; B, 368 RU; C, 720 RU; D, 1156 RU; E, 1998 RU; F, 2700 RU, respectively. A streptavidin-derivatized sensor chip lacking the bound N- $\Delta$ 430 $\tau$  provided a blank control, and the subtracted data are shown. DnaB at 1  $\mu$ M diluted in HKGM buffer was injected over the six N- $\Delta$ 430 $\tau$  immobilized sensor chips for 4 min at 5  $\mu$ l/min. The schematic at right indicates that if the N- $\Delta$ 430 $\tau$  density on a sensor chip is so low that only one N- $\Delta$ 430 $\tau$  molecule binds each DnaB<sub>6</sub> molecule, the resultant interaction is too weak to be observed using this methodology. However, at higher densities of immobilized N- $\Delta$ 430 $\tau$ , multiple N- $\Delta$ 430 $\tau$  molecules bind each DnaB<sub>6</sub> molecule, and the resultant interaction is strong enough to be detected.

and 270  $\mu$ M of C(0) $\tau$  as monomer, within the density range of N- $\Delta$ 430 $\tau$  used in the density dependence experiment (Table III). The observed binding ratio of DnaB<sub>6</sub> to C(0) $\tau$ <sub>4</sub> was 0.69, which was not significantly different from the ratio obtained when using with 2025 RU of C(0) $\tau$  (Table III).

#### DISCUSSION

In the preceding paper, we detailed our use of limited proteolysis studies to identify five putative structural domains of the  $\tau$  protein (15). Domains I–III are common to both  $\tau$  and  $\gamma$ . Domain IV is composed of 17 amino acid residues from the C-terminal end of  $\gamma$  plus 66 amino acids from the unique C terminus of  $\tau$ . Domain V is located at the C-terminal end of  $\tau$ . One function of  $\tau$  is to bind DnaB, coupling the holoenzyme with the primosome at the replication fork. C- $\tau$ , the unique C terminus of  $\tau$ , bound DnaB in a coupled immunoblotting method (12). In reconstituted rolling circle replication reactions, C- $\tau$  can partially replace full-length  $\tau$  in coupling the leading strand polymerase with the DnaB helicase at the replication fork (12).

This study further defined the DnaB binding domain of  $\tau$  by analyzing the interactions of DnaB with several truncated  $\tau$  proteins. N- $\Delta$ 413 $\tau$ , N- $\Delta$ 430 $\tau$ , C- $\Delta$ 147 $\tau$ , and C(0) $\tau$  bound DnaB with similar apparent  $K_d$  values. Because complicated binding kinetics were operative, the apparent  $K_d$  values we obtained in this study were not the true constants. However, the resulting apparent  $K_d$  values presumably contain the same systematic errors and therefore permit a quantitative comparison of relative affinities. The relative binding affinities of the different  $\tau$  fusion proteins for DnaB indicate that  $\tau$  amino acid residues 431–496 are sufficient for DnaB binding. This 66-residue stretch corresponds to the C-terminal portion of  $\tau$  domain IV.

Although similar apparent  $K_d$  values were obtained for the interactions of DnaB<sub>6</sub>-C(0) $\tau$ <sub>4</sub> and DnaB<sub>6</sub>-(N- $\Delta$ 430 $\tau$ )<sub>1</sub>, the binding ratios for the DnaB<sub>6</sub>-(N- $\Delta$ 430 $\tau$ )<sub>1</sub> was density-dependent. We conclude that more than one N- $\Delta$ 430 $\tau$  monomer is required to bind DnaB<sub>6</sub> and that the interactions between DnaB and  $\tau$  involved multivalent binding. Thus, the true microscopic  $K_d$  for binding of DnaB<sub>6</sub> to a single N- $\Delta$ 430 $\tau$  was too weak to observe using a BIAcore. At higher N- $\Delta$ 430 $\tau$  densities, binding was observed between DnaB<sub>6</sub> to two or more N- $\Delta$ 430 $\tau$  molecules; the observed macroscopic  $K_d$  is roughly equal to the product of each of the constituent microscopic  $K_d$  values.<sup>2</sup>

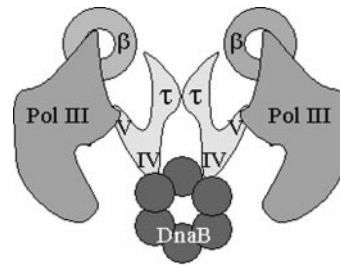


FIG. 5. **Both the leading and lagging strand polymerases couple the DnaB helicase via  $\tau$  at the replication fork.** The dimeric  $\tau$  protein binds the leading and lagging strand polymerases through domain IV. The two domain IVs of the dimeric  $\tau$  protein also bind a hexameric DnaB molecule at the replication fork. This double polymerase tether proceeding through  $\tau$ - $\tau$  and  $\tau$ -DnaB interactions helps keep the lagging strand associated with the replication fork and may serve to help retarget the dissociated lagging strand polymerase to the next primer synthesized at the replication fork.

Consistent with this interpretation, the number of DnaB<sub>6</sub> binding to a BIAcore chip surface increases with the density of immobilized N- $\Delta$ 430 $\tau$ . Increases in N- $\Delta$ 430 $\tau$  density would result in increased numbers of N- $\Delta$ 430 $\tau$  molecules becoming located within each DnaB<sub>6</sub> binding sphere. The DnaB<sub>6</sub> binding sphere is a function of the diameter of the distance between two binding sites within each DnaB<sub>6</sub> molecule. Within each binding sphere, a certain number ( $n$ ) of N- $\Delta$ 430 $\tau$  molecules can be accommodated;  $n$  is equal to the maximum potential binding stoichiometry of N- $\Delta$ 430 $\tau$  to DnaB<sub>6</sub>.

Recently, a model for quantifying the principal aspects of multivalent binding was developed (19). We used this model to estimate the probability of more than one N- $\Delta$ 430 $\tau$  molecules binding DnaB simultaneously. The proportion of spheres containing a given number of N- $\Delta$ 430 $\tau$  molecules was calculated assuming a binomial distribution. The DnaB-binding sphere was defined as the volume within which binding of the DnaB by two N- $\Delta$ 430 $\tau$  molecules can occur, and it was calculated using the following equation:  $V_S = 4/3 * \pi * D^3$ , where  $D$  is the distance between two binding sites on DnaB. The DnaB hexamer is a cyclic structure and contains six chemically identical subunits (14, 20, 21). Based on hydrodynamic and electron microscopic studies, the cyclic structure of the DnaB hexamer has an outside diameter of  $\sim$ 140  $\text{\AA}$  and an inner channel of  $\sim$ 40  $\text{\AA}$ . The

<sup>2</sup> Assuming that the 8 nm apparent  $K_d$  resulted from (N- $\Delta$ 430 $\tau$ )<sub>2</sub>-DnaB<sub>6</sub> interactions, the affinity between DnaB and each monomeric

N- $\Delta$ 430 $\tau$  would be in the 900  $\mu$ M range provided that there was no cooperativity involved ( $(8 \text{ nm})^{1/2} = 900 \mu\text{M}$ ). This low (900  $\mu$ M) affinity range is consistent with the lack of detected interaction.

expected DnaB binding sphere would be in the range from  $4/3 \cdot \pi \cdot (40 \text{ \AA})^3$  to  $4/3 \cdot \pi \cdot (140 \text{ \AA})^3$  (268–11480 nm<sup>3</sup>, respectively). If we assume that the interaction between  $\tau$  and DnaB involves two N- $\Delta$ 430 $\tau$  molecules, the calculated DnaB binding sphere is 2500 nm<sup>3</sup>, within the possible range for an interaction between two  $\tau$  protomers and DnaB<sub>6</sub>.

The notion that two  $\tau$  protomers bind each DnaB hexamer is consistent with the presence of a  $\tau$  dimer at the replication fork (Fig. 5).  $\tau_2$  functions to dimerize the DNA polymerase III core to enable simultaneous synthesis of leading and lagging strands. We already know that the leading strand polymerase is tethered to DnaB (12). The findings presented in this report indicate that the same DnaB molecule couples both of the leading and lagging strand polymerases. Thus, a double tethers exists between the leading and lagging strand polymerase, one is through the  $\tau$ - $\tau$  link and the additional one through the  $\tau$ -DnaB link. This second tether might help keep the lagging strand associated with the replication fork and may serve to help retarget the dissociated lagging strand polymerase to the next primer synthesized at the replication fork (Fig. 5). Our mapping results demonstrate that the DnaB helicase binds  $\tau$  domain IV and that the polymerase  $\alpha$  subunit binds domain V (15). These findings indicate important roles that the C terminus  $\tau$  plays in DNA synthesis.

## REFERENCES

1. McHenry, C. S. (1988) *Annu. Rev. Biochem.* **57**, 519–550
2. McHenry, C. S. (1991) *J. Biol. Chem.* **266**, 19127–19130
3. Kelman, Z., and O'Donnell, M. (1995) *Annu. Rev. Biochem.* **64**, 171–200
4. McHenry, C. S., Griep, M. A., Tomaszewicz, H., and Bradley, M. (1989) in *Molecular Mechanism in DNA Replication and Recombination*, pp. 115–126, Alan R. Liss, Inc., New York
5. Flower, A. M., and McHenry, C. S. (1990) *Proc. Natl. Acad. Sci. U. S. A.* **87**, 3713–3717
6. Blinkowa, A. L., and Walker, J. R. (1990) *Nucleic Acids Res.* **18**, 1725–1729
7. Tsuchihashi, Z., and Kornberg, A. (1990) *Proc. Natl. Acad. Sci. U. S. A.* **87**, 2516–2520
8. McHenry, C. S. (1982) *J. Biol. Chem.* **257**, 2657–2663
9. Studwell-Vaughan, P. S., and O'Donnell, M. (1991) *J. Biol. Chem.* **266**, 19833–19841
10. Kim, S., Dallmann, H. G., McHenry, C. S., and Mariani, K. J. (1996) *Cell* **84**, 643–650
11. Yuzhakov, A., Turner, J., and O'Donnell, M. (1996) *Cell* **86**, 877–886
12. Dallmann, H. G., Kim, S., Mariani, K. J., and McHenry, C. S. (2000) *J. Biol. Chem.* **275**, 15512–15519
13. Reha-Krantz, L. J., and Hurwitz, J. (1978) *J. Biol. Chem.* **253**, 4043–4050
14. Bujalowski, W., Klonowska, M. M., and Jezewska, M. J. (1994) *J. Biol. Chem.* **269**, 31350–31358
15. Gao, D., and McHenry, C. S. (2000) *J. Biol. Chem.* **275**, 4433–4440
16. Kim, D. R., and McHenry, C. S. (1996) *J. Biol. Chem.* **271**, 20690–20698
17. Cull, M. G., and McHenry, C. S. (1995) *Methods Enzymol.* **262**, 22–35
18. Dallmann, H. G., Thimmig, R. L., and McHenry, C. S. (1995) *J. Biol. Chem.* **270**, 29555–29562
19. Muller, K. M., Arndt, K. M., and Pluckthun, A. (1998) *Anal. Biochem.* **261**, 149–158
20. San Martin, M. C., Stamford, N. P., Dammerova, N., Dixon, N. E., and Carazo, J. M. (1995) *J. Struct. Biol.* **114**, 167–176
21. Yu, X., Jezewska, M. J., Bujalowski, W., and Egelman, E. H. (1996) *J. Mol. Biol.* **259**, 7–14